



# CityZen

megaCITY - Zoom for the Environment

Collaborative Project

*7th Framework Programme for Research and Technological Development*

**Cooperation, Theme 6:**

**Environment (including Climate Change)**

Grant Agreement No.: 212095

## Deliverable D2.2.1, type R

**Report on high-temperature impact on BVOC emissions and air quality for the summer 2003 case**

Due date of deliverable: project month 12  
Actual submission date: project month 36

Start date of project: 1 September 2008  
Name of lead beneficiary for this deliverable:  
Scientist(s) responsible for this deliverable:

Duration: 36 months  
NILU  
Sverre Solberg (NILU), Tove Svendby (NILU),  
Øivind Hodnebrog (UiO), Andreas Hilboll  
(IUP-UB)

<b>Project co-funded by the European Commission within the Seventh Framework Programme (2007-2013)</b>		
<b>Dissemination Level</b>		
PU	Public	X
PP	Restricted to other programme participants (including the Commission Services)	
RE	Restricted to a group specified by the consortium (including the Commission Services)	
CO	Confidential, only for members of the consortium (including the Commission Services)	

## **1 Report on high-temperature impact on BVOC emissions and air quality for the summer 2003 case**

When the project application was written this deliverable was focused on the heat wave and extreme pollution event in summer 2003 in W-Europe. At the time of project start a large number of scientific studies concerning the 2003 episode had already emerged (Emmerson et al., 2007; Solberg et al., 2008; Tressol et al., 2008; Curci et al., 2009). The CityZen consortium then suggested and got acceptance for moving the focus to the 2007 summer heat wave(s) in the Eastern Mediterranean and, furthermore, to adopt a broader, more general perspective.

The present deliverable report is split into two: One part is dedicated to the study of the heat waves in the East Mediterranean (hereafter denoted EM) hot spot in summer 2007, and these results will be published in Hodnebrog et al. 2011b (in preparation). The other part concerns fine scale model studies for the Po Valley hot spot using a nested model system with newly developed routines for secondary organic aerosols (SOA) formation. The report gives an overview of the relationship between meteorological drivers (such as temperature) and secondary species (such as ozone, BVOC and aerosols) as seen from this modeling.

### **1.1 Description of the chemical transport models used**

#### ***1.1.1 The unified EMEP model – introducing a nested WRF/EMEP system***

The Unified EMEP model (Simpson et al., 2003) is a chemical transport model developed at the Meteorological Synthesizing Centre - West (MSC-W) at the Norwegian Meteorological Institute (met.no). It is a terrain following sigma coordinate model designed to calculate air concentration and deposition fields for acidifying and eutrophying compounds, ground level ozone, and particulate matter, as well as their long-range transport and fluxes across national boundaries.

The current EMEP model version, and the provided gridded input data, have a standard horizontal resolution of 50 x 50 km<sup>2</sup> (at 60°N) and are defined on a polar stereographic projection with 20 sigma levels vertically. The model is flexible with regard to the horizontal resolution, and in CityZen the EMEP model has been run on the standard 50 km as well as 25 km, 10 km and 2.5 km grid scales. The PARLAM-PS numerical weather prediction model is used to generate standard meteorological data for the EMEP model every 3 hours. Other models, such as WRF, can also be used to provide the necessary meteorological fields, and that was done within CityZen WP2.2, as explained below. The vertical resolution in the EMEP model is currently restricted to the fixed 20 layer system. Detailed description of the model is given in the EMEP Status Report 1/2003 Part I (Simpson et al., 2003).

One objective of CityZen was to use the EMEP Unified model to study the scale-dependency of photochemical processes and in particular reactions between anthropogenic NO<sub>x</sub> from megacities and biogenic VOC from surrounding areas. These components are important for the formation of ozone and secondary organic aerosols (SOA) around megacities, particularly in southern locations such as the Po Valley and the East Mediterranean. Such a study required a nested EMEP model.

To facilitate this, a combined WRF-EMEP modeling system was developed through WP2.2 in CityZen. This modeling system was similar to the “EMEP4UK” (the application of the EMEP unified model for the UK) as documented by Vieno et al., 2010. We designed the WRF model to produce meteorological fields on 50 km, 10 km and 2.5 km, respectively, and these fields were input to the EMEP unified model. WRF was run for the full EMEP domain with the 50 km resolution and for a large and small Po Valley domain for the 10 km and 2.5 km nests, respectively. Initial and boundary conditions of the chemical trace species were successively fed from the larger

domain to the smaller one. All the nested EMEP model runs were done for 2006 as we then had EMEP's HIRLAM 10 km meteorological data to compare with the WRF 10 km data.

Additionally, new state-of-the-art routines for biogenic emissions and formation of secondary organic aerosols (SOA) were developed for the EMEP model by met.no in parallel with the CityZen project. These routines were eventually made available for WP2.2 in CityZen. Thus, a fine-scale nested EMEP modeling system with state-of-the-art SOA routines were run for the first time through the CityZen project. Details about the routines for biogenic emissions and SOA formation are given in the technical appendix at the end of this report.

### ***1.1.2 The WRF-Chem model***

The Weather Research and Forecasting model with Chemistry (WRF-Chem) (Grell et al., 2005) consists of a mesoscale meteorological model (WRF) (Skamarock and Klemp, 2008) coupled with a chemistry module. In this study, WRF-Chem version 3.2 has been used with the RADM2 (Stockwell et al., 1990) gas-phase chemistry scheme.

The modules and meteorological physics schemes are the same as in Hodnebrog et al. (2011a), but the following modification has been done to the FTUV (Madronich, 1987) photolysis scheme: For each day in the simulation, the model reads a domain-averaged total O<sub>3</sub> column value that is calculated by the global Oslo CTM2 model (Søvde et al., 2008) using a simulation setup described in Colette et al. (2011), and this value is then used in the calculation of photolysis rates. Meteorological initial and boundary conditions are used from ECMWF-IFS model analysis at a resolution of 0.25° × 0.25° and updated every 6 hours. Furthermore, meteorological parameters calculated by WRF are nudged towards the ECMWF-IFS data every time step. Initial and boundary conditions for the chemical species are updated every 6 hours from results obtained with the Oslo CTM2 model.

The WRF-Chem model domain is centered over the Balkan Peninsula, covers most of the Mediterranean Sea in the south, and extends up to mid-Germany in the north, while the EMEP model domain is much larger, covering all of Europe (Figure 1).

### ***1.1.3 Anthropogenic emissions***

The emissions in the Unified EMEP model and WRF-Chem have several similarities. In both models, the anthropogenic emissions are based on the country total emissions officially reported to EMEP, but the methods used to grid the emissions to fine scale are different. In WRF-Chem the TNO/EMEP emission inventory (Kuenen et al., 2010) has been used, which has a resolution of 1/8° longitude x 1/16° latitude (approximately 7 km x 7 km). Next, a splitting of the total NMVOC was made based on the UK emissions of the 50 most significant NMVOC species (Dore et al., 2007). Source-dependent factors were applied to obtain lumped species for the RADM2 chemistry scheme. In the EMEP model the emissions are provided for 10 anthropogenic source-sectors (SNAP sectores) and 1 sector which includes natural and biogenic emission sources. The emission data are available from <http://www.emep.int> and further details can be obtained at that site. For both EMEP and WRF-Chem monthly and daily time factors are applied to the emission data. More details about the EMEP emission input can be found in Simpson et al., 2003.

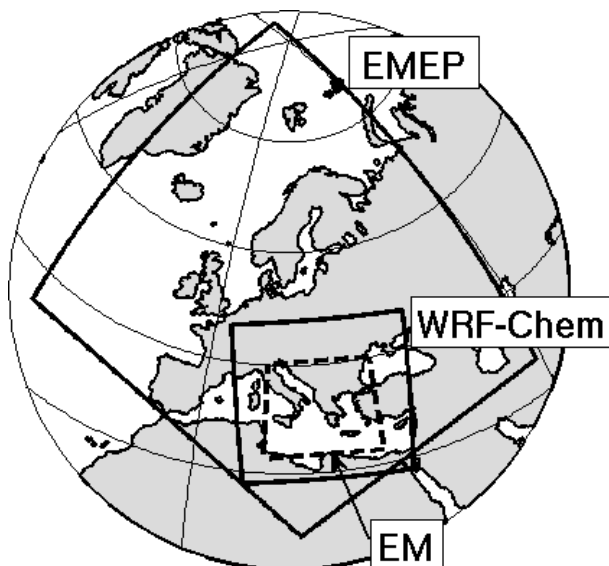


Figure 1. Locations of the domains used in the EMEP and WRF-Chem simulations, and of the common domain covering most of the Eastern Mediterranean.

#### 1.1.4 Forest fire emissions

Forest fires turned out to be an important contribution to the atmospheric pollution level during the East Mediterranean heat waves in summer 2007. Thus, such emissions had to be included in the WRF and EMEP models. Forest fire emissions were taken from the Global Fire Emission Database version 2 (GFEDv2) (van der Werf et al., 2006) and from the newly developed Fire INventory from NCAR version 1 (FINNv1) (Wiedinmyer et al., 2011). The temporal and spatial resolutions differs substantially between the two inventories; the first providing  $1^\circ \times 1^\circ$  gridded data for every 8<sup>th</sup> day, whereas the latter provides daily emissions with a  $1 \text{ km} \times 1 \text{ km}$  resolution. The total emissions by each inventory for the summer 2007 forest fires in the East Mediterranean are also quite different, at least for  $\text{NO}_x$  and CO, showing higher emissions in the GFEDv2 inventory compared to FINNv1. One of the most intense forest fire episodes took place between July 20 – 31, when fires broke out both in Peloponnese in Greece, and along the coast of Croatia. Around August 21, new intense fires emerged, mainly in south Greece, and continued into early September.

#### 1.1.5 Biogenic emissions

Biogenic emissions are calculated online in both the EMEP and WRF models, and are dependent on land-use data and weather conditions. In WRF-Chem, the Model of Emissions of Gases and Aerosols from Nature (MEGAN) version 2.04 (Guenther et al., 2006) is dependent on ambient temperature, photosynthetic active radiation, humidity, wind speed and soil moisture when estimating emissions of isoprene, monoterpenes, other biogenic VOCs, and nitrogen emissions from soil. In the EMEP model biogenic emissions of isoprene and monoterpenes are calculated for every grid-cell, and at every model timestep, using near-surface air temperature ( $T_2$ ) and photosynthetically active radiation (PAR), the latter being calculated from the model's solar radiation, modified by the total cloud fraction (CL). The underlying emission potentials, land-cover data bases, and model coding have changed substantially in the most recent EMEP model version. The appendix describes this in more detail.

The temporal evolution of biogenic isoprene emissions calculated by WRF-Chem and EMEP are very similar (Figure 2), but there is a difference in the magnitude and in the horizontal distribution of the emissions (Figure 3). The isoprene emissions calculated by WRF/MEGAN is systematically higher than by the EMEP model. These differences could be attributed to different emission factors

and land use classifications. In particular, MEGAN predicts large isoprene emissions from shrublands in the western part of Turkey and south Greece, and from broadleaf trees northwest on the Balkan Peninsula. The differences are, however, well within known uncertainties, which are at least a factor of 2 for natural emissions (Simpson et al., 1999).

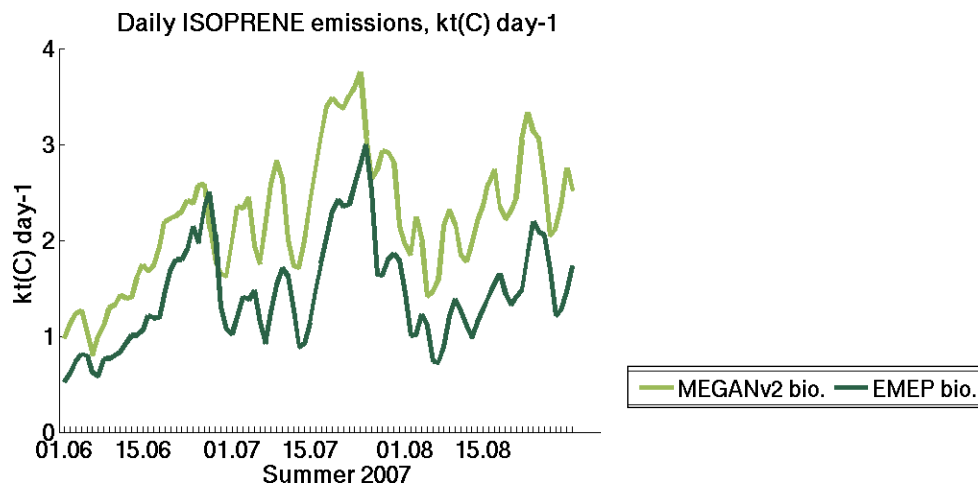


Figure 2. Temporal evolution of the calculated isoprene emissions from biogenic sources during summer 2007 (kilotons C day<sup>-1</sup>) summed over the East Mediterranean hot spot region from the WRF/MEGAN and the EMEP models, respectively.

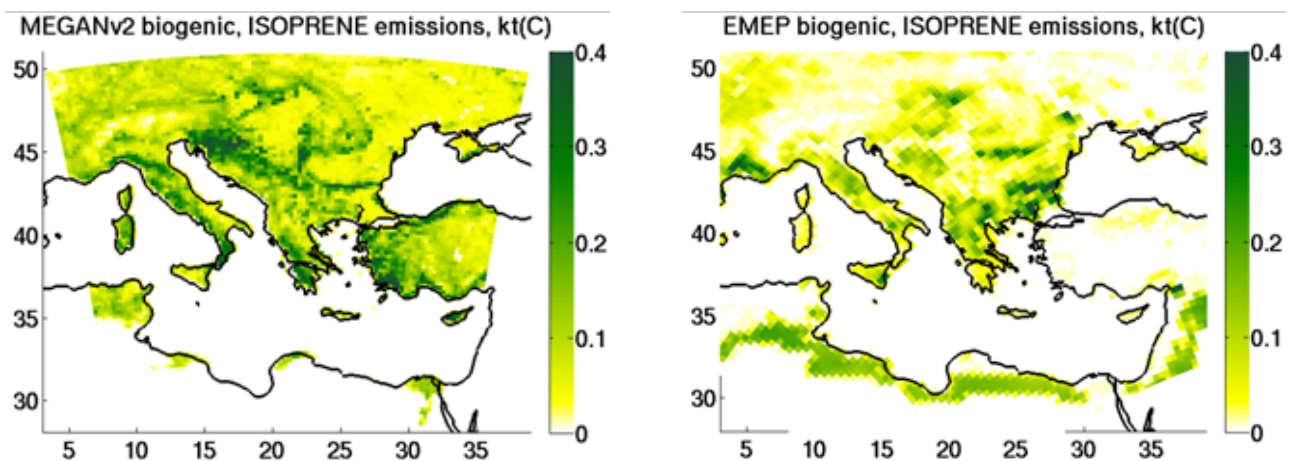


Figure 3. Emissions of isoprene used in the reference simulations of the WRF-Chem (left) and the EMEP Unified (right) models.

## 1.2 East Mediterranean heat wave 2007

### 1.2.1 Background

The Eastern Mediterranean (EM) is constantly exposed to air pollution problems due to its unique location and because of rapid urbanization (Kanakidou et al., 2011). Maximum ozone mixing ratios in and downwind of major urban areas in Greece are found to exceed the European Union (EU) health risk threshold level of 90 ppb (Poupkou et al., 2009). The region acts as a reservoir for anthropogenic pollutants originating from the nearby emission hot spots Cairo, Istanbul and Athens, from maritime transport emissions (Poupkou et al., 2008), and from more distant sources, particularly the European continent (Gerasopoulos et al., 2005). Additionally, biogenic emissions of isoprene, monoterpenes and other VOCs are large on the Balkan Peninsula, and represents 70-80 % of the annual total NMVOC emissions in most of the countries in this region (Symeonidis et al., 2008).

Three distinct heat waves combined with large emissions from forest fires led to elevated ozone and particulate matter (PM) levels in the EM region during the summer of 2007 (Eremenko et al., 2008; Liu et al., 2009). In Greece, more than 12 % of the forested area burnt (Kaskaoutis et al., 2011), contributing substantially to the air pollution levels in Athens (Liu et al., 2009). Extreme levels of carbon monoxide (CO) were observed from satellites, indicating up to 22 ppmv close to the fires and 4 ppmv in the transported plume above the Mediterranean Basin (Turquety et al., 2009). The Greek forest fires were the most extensive and destructive in the recent history of the country, and they were a consequence of several heat waves and long periods of drought (Founda and Giannakopoulos, 2009). In fact, several stations in Greece reported record breaking temperatures (up to 47°C), making this the hottest summer ever measured.

Tropospheric columns of O<sub>3</sub> calculated from the OMI total ozone column with the MLS stratospheric column subtracted (Ziemke et al., 2006) clearly confirm the existence of a positive ozone anomaly in the EM region in summer 2007 compared to other years (Figure 4).

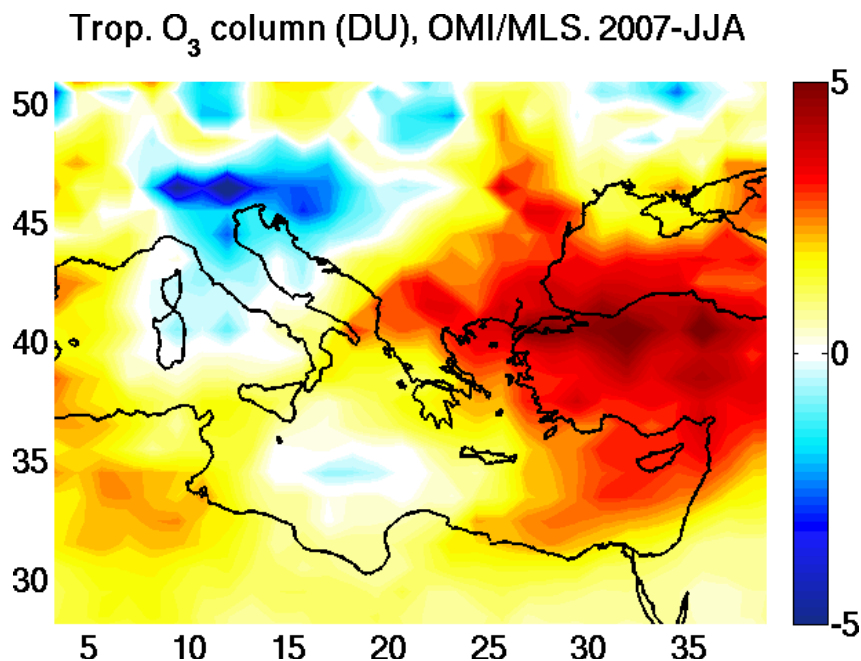


Figure 4. The difference in tropospheric O<sub>3</sub> column (DU) from OMI/MLS (<http://www.nasa.gov>) for the summer (June-July-August) 2007 compared to the mean of the summers 2005, 2006, 2008 and 2009.

### 1.2.2 Modeling

For each of the two models (EMEP Unified and WRF-Chem) one reference simulation and a number of sensitivity simulations were performed. The impact of fire emissions, biogenic emissions, anthropogenic emissions and dry deposition on ozone and BVOCs was investigated by turning off the respective emission sector (or process) in the sensitivity simulations. In addition sensitivity simulations were performed with temperatures restricted to maximum 28°C.

Unfortunately, there are very few background monitoring stations in the EM region to compare with. Most stations are located in urban or suburban locations, making them less suited for comparison with regional scale model calculations. Furthermore, the intensive fire plumes during the 2007 heat waves were mainly transported to the sea, thus not seen by the surface sites. Satellite measurements therefore proved to be most relevant for comparison with the modeling results.

Figure 5 shows the tropospheric column of NO<sub>2</sub> for 24-26 August 2007 as retrieved by the OMI satellite instrument and modeled with WRF and EMEP. The fires plumes are clearly seen in the satellite data and also reflected fairly well in the modeling data. Emissions from fires are necessarily very uncertain. The uncertainty regards both the spatial and temporal variation as well as the absolute magnitude and the emission intensity. Given this uncertainty, the models capture the location and the influence of the fires surprisingly well.

Biogenic emissions are closely dependent on temperature and solar radiation. During heat waves such as the EM 2007 episodes, biogenic emissions of isoprene and terpenes may contribute significantly to the formation of ozone and aerosols. A sensitivity run without biogenic emissions was carried out for the two models reported here, and the difference compared to the standard run is shown in Figure 6. Even in the 3-months mean summer concentration the influence of biogenic emissions are calculated to contribute significantly to ozone; up to 10 ppbv in certain areas. The results indicate a larger effect in the WRF-Chem model compared to EMEP Unified. This difference could be explained by the difference in the total isoprene emissions (Figure 3) in the two models. As mentioned, the isoprene emissions in the WRF-Chem model are significantly higher than in EMEP Unified. This model-to-model difference is seen overall, and is particularly apparent in the eastern area (Turkey) due to the largest difference in emissions there.

A similar model sensitivity study keeping the temperature below 28°C caused a similar pattern, although much lower in magnitude. As the isoprene emission is controlled by temperature (and solar radiation) a main temperature effect on ozone is through the biogenic isoprene emissions, being larger in WRF-Chem than in the EMEP Unified model.

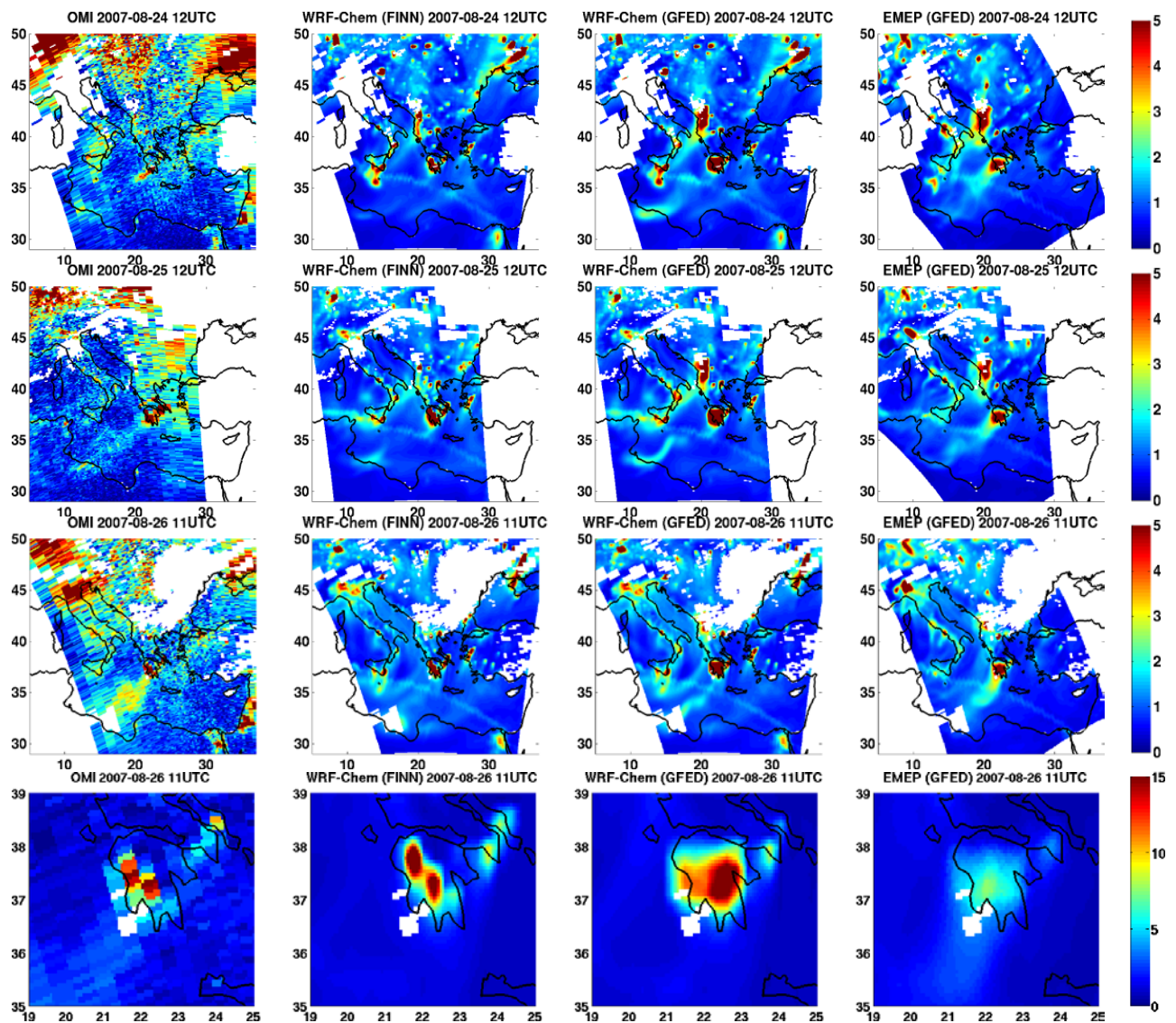


Figure 5. Tropospheric columns of  $\text{NO}_2$  ( $10^{15}$  molec  $\text{cm}^{-2}$ ) as retrieved from the OMI satellite instrument (1<sup>st</sup> column), and as modelled with the WRF-Chem (2<sup>nd</sup> and 3<sup>rd</sup> columns) and EMEP (4<sup>th</sup> column) models for August 24 (1<sup>st</sup> row), 25 (2<sup>nd</sup> row), and 26 (3<sup>rd</sup> and 4<sup>th</sup> rows) in 2007. In the second column, FINN forest fire emissions have been used in the simulations, while in the two rightmost columns, GFED emissions have been used. The bottom plots have different color scale and are zoomed in on the Peloponnese fires.

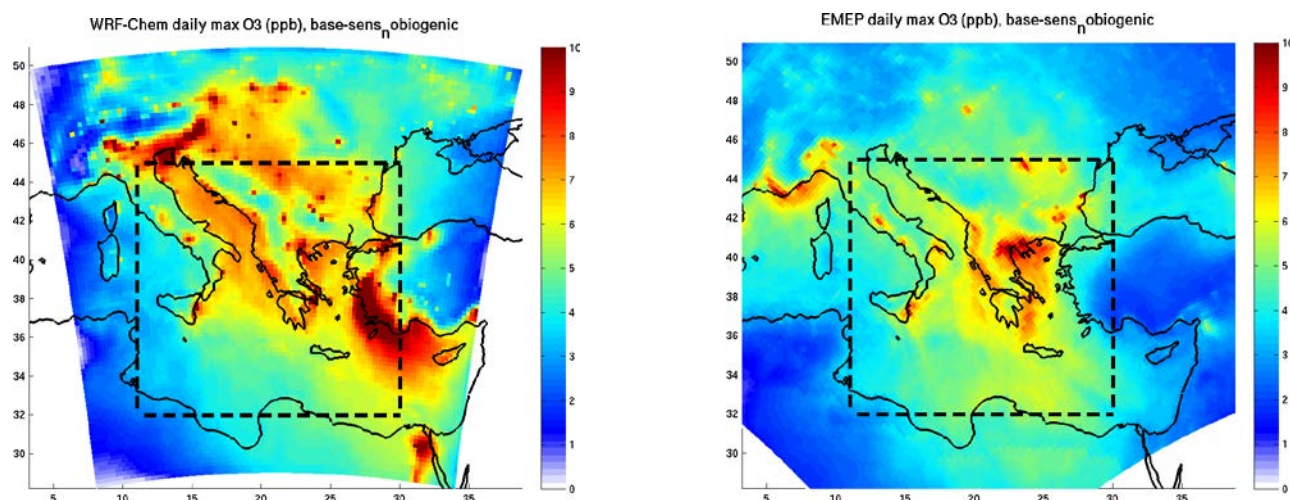


Figure 6. Change in daily maximum near-surface ozone ( $\Delta$ ppb) due to biogenic emissions calculated by WRF-Chem (left) and EMEP (right) averaged over the period 1 June – 31 August 2007.

### 1.3 Case study Po Valley

Po Valley is one of the defined hot spot regions in the CityZen project. A significant effort in WP2.2 has been to carry out fine scale CTM calculations to evaluate the influence of biogenic and anthropogenic emissions for ozone and PM in this region. The mixing between biogenic and anthropogenic emissions and the response of elevated temperatures on the photochemistry has been some of the issues studied. In order to do this a certain model development was necessary. The following chapters give an overview of this development, followed by a chapter presenting the main findings and conclusions of relevance for CityZen.

The standard EMEP model (Simpson et al., 2003) was available at the beginning of CityZen. However, as stated in CityZen's DoW, calculations of biogenic and anthropogenic tracers using a nested EMEP model system on a fine spatial scale was needed in CityZen WP2.2. Thus, two types of model development were carried out: Introducing nesting in the EMEP model and, secondly, refinement of the modeling of biogenic emissions and their photochemistry.

For the nested model studies we have focused on the summer 2006, since both 50 km and 10 km resolution Parlam/Hirlam meteorological data are available for this specific year. In addition to the standard EMEP input files we have used WRF to generate meteorological input data on three nests: a) 50 km (EMEP domain), b) 10 km (large Po Valley region), and c) 2.5 km (small Po Valley region). The WRF simulations are based on meteorological data from NCEP (National Centers for Environmental Prediction), NOAA National Weather Service. The WRF model can be run with various sets of physical and chemical parameterizations and we have chosen a setup similar to the one used by Vieno et al. (2010). The WRF output files were converted to EMEP compatible meteorological input files with software developed at met.no.

Emission data were required for the three model nests described above. Official emission data for  $\text{NO}_x$ , VOC, CO and  $\text{SO}_x$  were available for 2006 from EMEP for 50 km and 10 km resolution for the whole EMEP domain. In addition emission data for the smallest domain, covering the Po Valley region, were needed on a 2.5 km resolution. For this purpose data from the POMI project for 2005 on a 3 km resolution (Thunis et al., 2009) were made available to us. The POMI data were given on a UTM coordinate system and had to be regridded to our EMEP 2.5 km polar stereographic domain. All technical details about the regridding procedure are not given here. In short, we split the 2.5 km grid cells into a number of smaller cells and picked the closest POMI grid for every sub-cell. In

addition, it was required that the total emission for every 10 km grid cell (i.e. 4x4 grid cells of 2.5 km size) should equal the official EMEP 10 km emission data. This procedure was followed for every emission compound and every SNAP sector. The POMI data contained gridded data, representing area and line sources, as well as point source data. For convenience, the POMI point source data was not used in the regridding of the emission data. As an example Figure 7 shows the annual emissions of NO<sub>x</sub> from traffic for the EMEP 50 km and 10 km grid cells, as well as the 3 km POMI data and the regridded 2.5 km data used in CityZen.

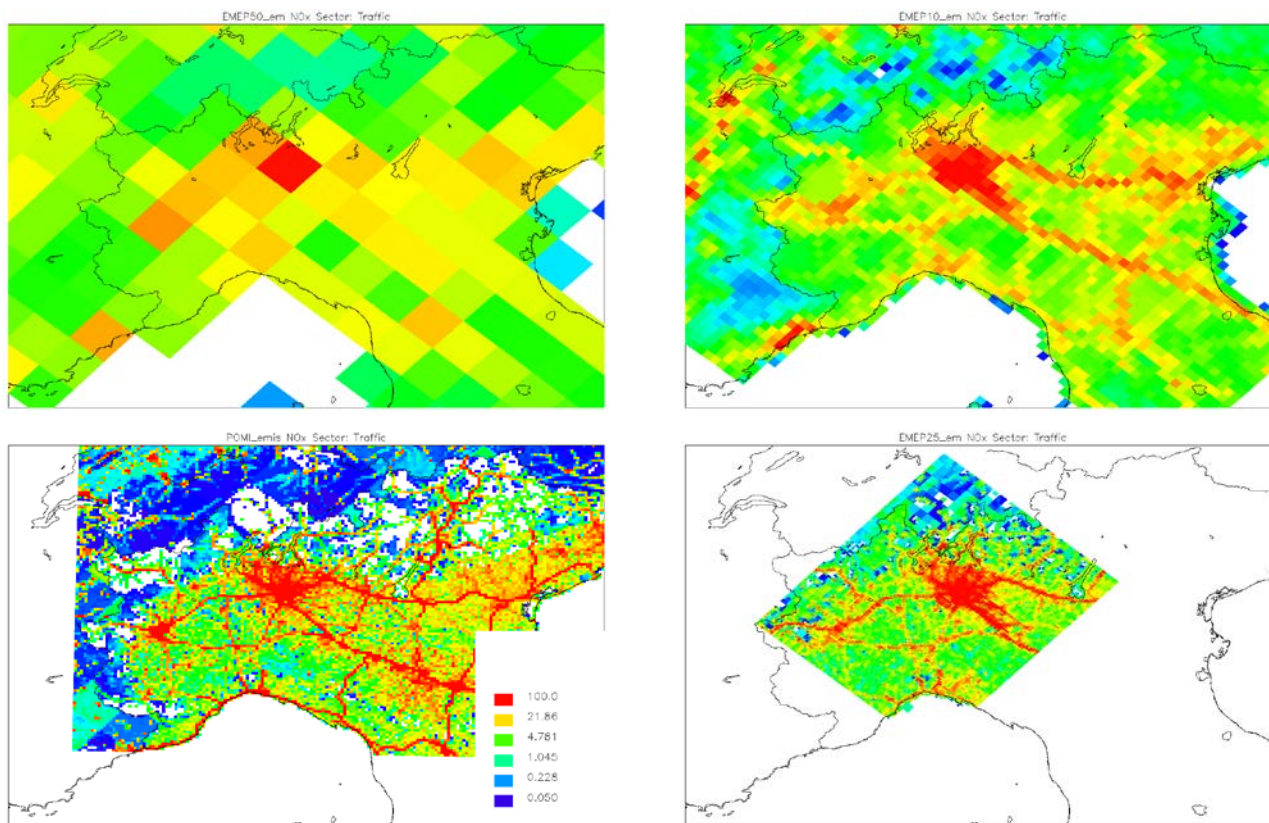


Figure 7. Annual emissions of NO<sub>x</sub> from traffic (SNAP sector 7) from the EMEP 50 km, EMEP 10 km, POMI 3 km and EMEP 2.5 km grid systems. The color scale indicates the emissions in g m<sup>-2</sup> for the POMI grid.

#### 1.4 Results from nested model studies for the Po Valley with the new SOA/VBS scheme

The nested model system described above was applied for the Po Valley hot spot region defined within CityZen. The combined EMEP/WRF model system was used to provide results for three nests with a 50 km, 10 km and 2.5 km spatial resolution, respectively. Emissions of biogenic trace species (isoprene and terpenes) were included as explained in the technical appendix below in addition to the anthropogenic emissions of NO<sub>x</sub>, SO<sub>x</sub>, VOC and CO. The 50 km results were used as boundary and initial concentrations for the 10 km domain, which in turn were used as boundary and initial concentrations for the 2.5 km domain. The model system was run for the period June–August 2006, as we then also had access to 10 km meteorological data from the HIRLAM model.

Figure 8 shows the average surface concentrations modeled for July 2006 for the 10 km and 2.5 km nests for BSOA (biogenic secondary organic aerosols) in the same color scale and for the same geographical area. The results for the 2.5 km nest give finer details compared to the 10 km nest, corresponding to the finer resolution of the topography and land use. Overall, however, the results

for the two nests do not indicate large differences in these monthly mean values. The spatial distribution, min and max values are comparable for the two nests.

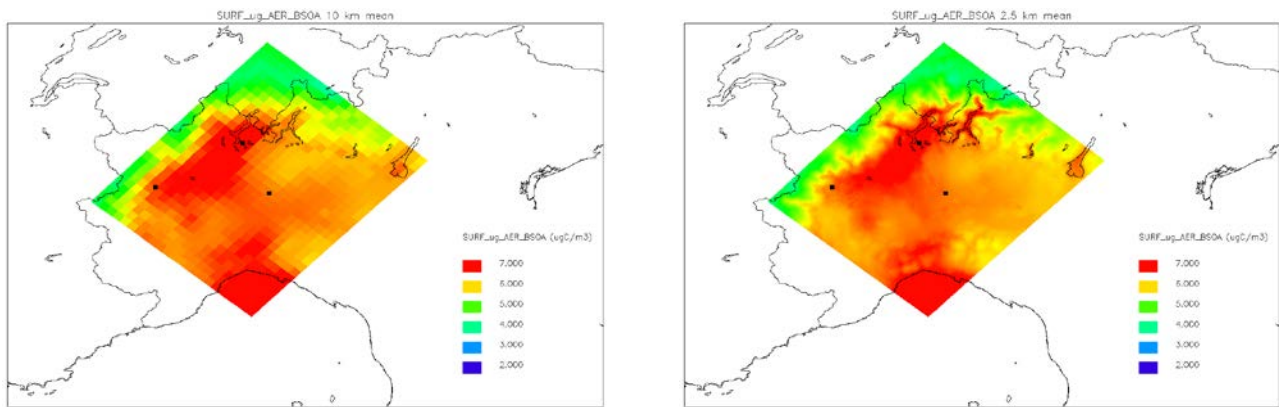


Figure 8. Modeled monthly mean concentrations of BSOA in the 10 km nest (left) and the 2.5 km nest (right). The color scale are the same and shows the values in  $\mu\text{g} (\text{C}) \text{m}^{-3}$ .

The relative differences in modeled monthly mean concentration for July 2006 between the two nests are given in Figure 9. Differences of the order of  $\pm 5\%$  are found. This is a surprisingly small difference given the substantial uncertainty in the actual BSOA concentrations. The reason why we don't see larger differences in the model results could be that the underlying data for temperature, solar radiation and land cover, which determines the emissions of the primary biogenics (isoprene and terpenes) do not show a very fine scale pattern.

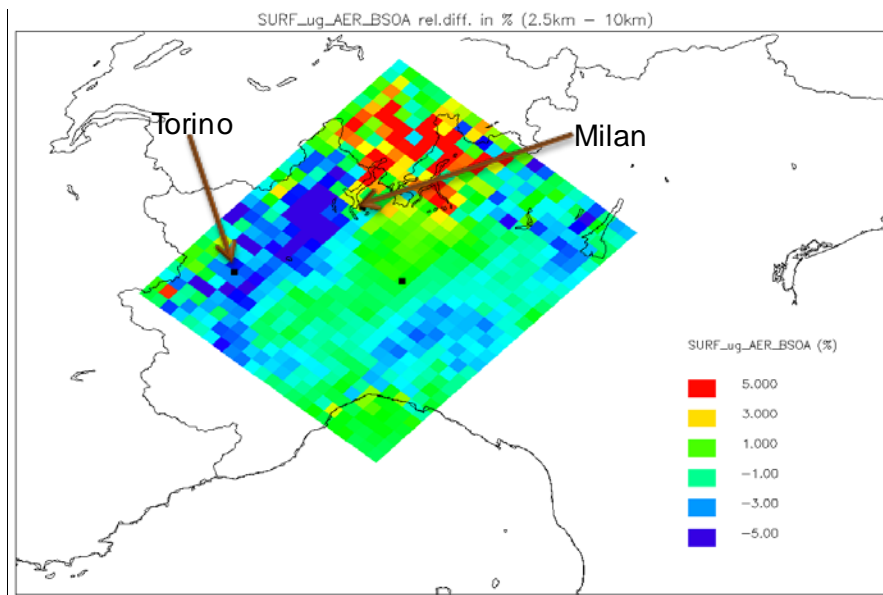


Figure 9. Relative difference in the mean surface concentration of BSOA for July 2006 calculated with the 10 km nest and the 2.5 km nest. Unit: %.

Figure 10 shows the relationship between the calculated BSOA concentrations in the 10 km nest compared to the 2.5 km nest as a scatter plot. In this figure each 10 km grid cell is shown as 16 identical BSOA values which are compared against the 16 different 2.5 km BSOA values in that 10 km grid square. This figure confirms the small differences in modeled BSOA for the two different grid resolutions. The results indicate a slight decrease in modeled BSOA in the 2.5 km nest for the

highest concentrations, i.e. a slight non-linear effect giving reduced BSOA for the highest peak episodes, but the effect is not very large.

Time series of surface BVOC for a point in the Milan area and the Torino area as modeled with the 50 km, 10 km, and 2.5 km for June-August 2006 are given in Figure 11. The location of these points is shown as black dots on the map in Figure 9. For the point in the Milan area the time series for all three nests follow each other closely, except for a period in the last part of June. Somewhat larger differences are found for the point in the Torino area. There the results from the 50 km nest are mostly lower than for the other nests. Overall, the time series, as the monthly means shown above, are fairly similar throughout this summer period. We conclude that for this period, with the meteorological and land cover data used, the importance of model resolution is rather small. One should not, however, regard this as a general conclusion. Land use data of a finer spatial scale could cause larger differences in the calculated fields.

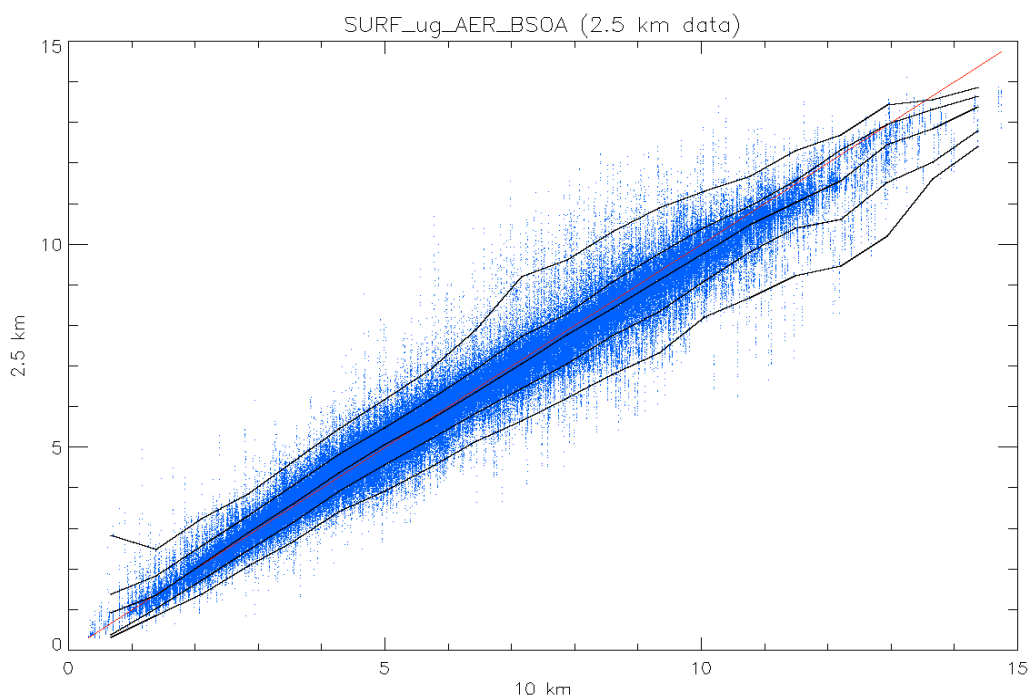


Figure 10. Scatter plot showing the relationship between the BSOA concentrations calculated for the grid squares from the 10 km nest and the 2.5 km nest (blue dots). The red line shows the 1:1 line and the black lines show the 1, 25, 50, 75 and 99 running percentiles. Unit:  $\mu\text{g m}^{-3}$ .

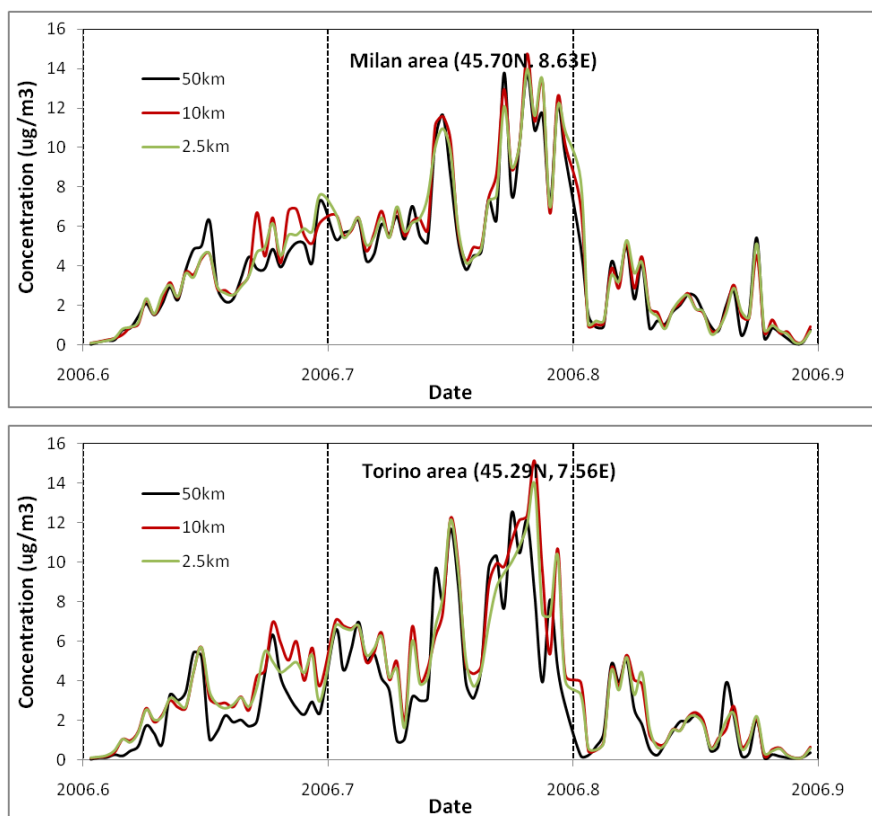


Figure 11. Hourly concentrations of surface BSOA for a point in the Milan area and the Torino area as modeled with the 50 km, 10 km, and 2.5 km for June-August 2006.

One aim of WP 2.2 was to study the effect of temperature on the formation of ozone and aerosols. A model sensitivity run was carried out with the temperatures increased by 5°C. The change in the surface concentration of ozone and BSOA for the 10 km nest is shown in Figure 12 for July 2006 as an average. An overall increase of 5°C gives a significant impact on the modeled concentration of aerosols and ozone. A surface ozone increase of more than 20% as a monthly mean in certain areas (actually outside the Po Valley itself) is found. The geographical pattern of the ozone change indicates that most of this increase is due to increased isoprene emissions. Isoprene is a major ozone precursor when NO<sub>x</sub> is present and the emissions are controlled by temperature and solar radiation. Additionally, a temperature increase of 5°C will lead to an overall speed-up of the atmospheric chemistry, a destabilization of PAN etc, which will contribute to an increase in the rate of formation of ozone and aerosols. The applied temperature increase leads to an increase in the BSOA concentrations by almost 40 % in the whole domain shown (except for sea areas).

The time series of the temperature scenario effect (Figure 13) indicates that increased ozone and BSOA are found more or less throughout the whole period. Largest effects are seen when there are peaks in these components, indicating that the high peak values are particularly sensitive to changes in temperatures. Smallest changes are found in August. For BSOA there is almost no change in the BSOA concentrations for the Torino site in the +5 °C scenario in August.

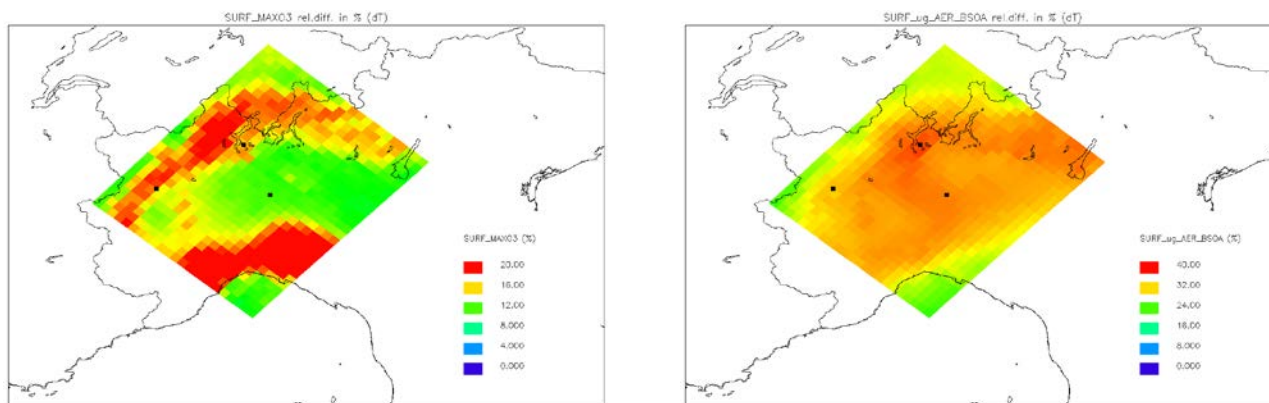


Figure 12. Modeled change in the mean concentrations for July 2006 for daily max ozone (left) and BSOA (right) due to a temperature increase of 5 °C. The nest with 10 km resolution is shown. Note that the color scales differ.

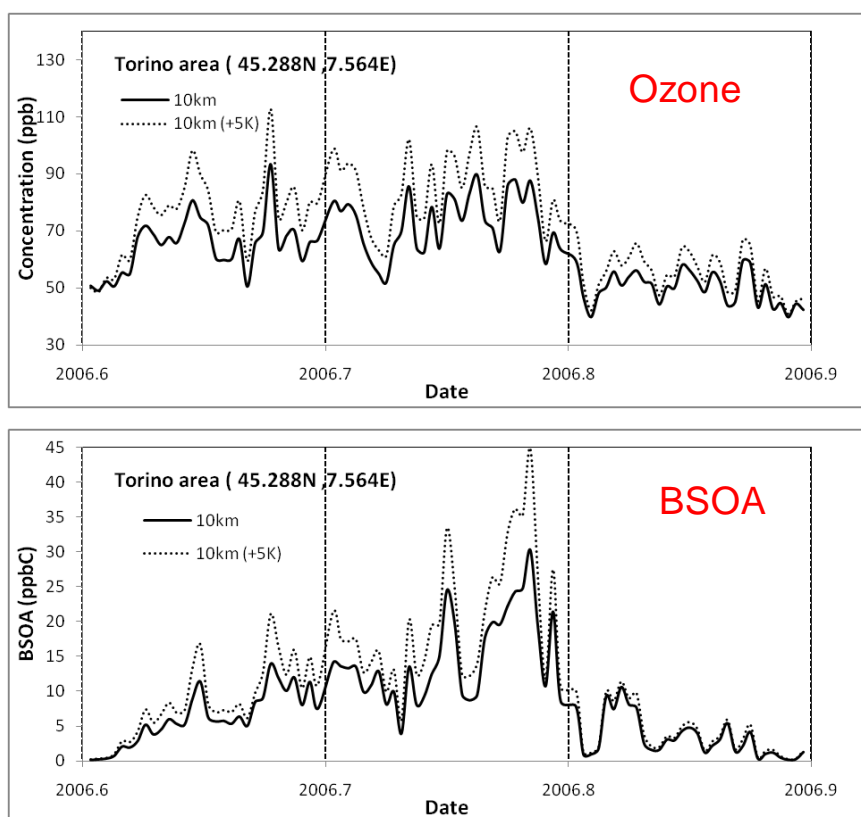


Figure 13. Hourly concentrations of surface ozone and BSOA for a point in the Milan area and the Torino area as modeled with the 10 km nest for June-August 2006. The time series show the standard scenario and a scenario with a 5 °C increase in temperature.

Largest effect of the +5 °C scenario is found for isoprene (Figure 14) which shows a doubling in the mean July 2006 concentration in the region north of the Po Valley. Comparing this field with the modeled ozone (Figure 12), clearly indicates that increased isoprene emission (due to increased temperature) is the main cause for the ozone increase modelled.

The mean PM<sub>2.5</sub> concentration is found to increase by more than 20% in a large part of the area shown, although not in the main area of the Po Valley. Again, this increase is to a large extent caused by increases in the biogenic precursors.

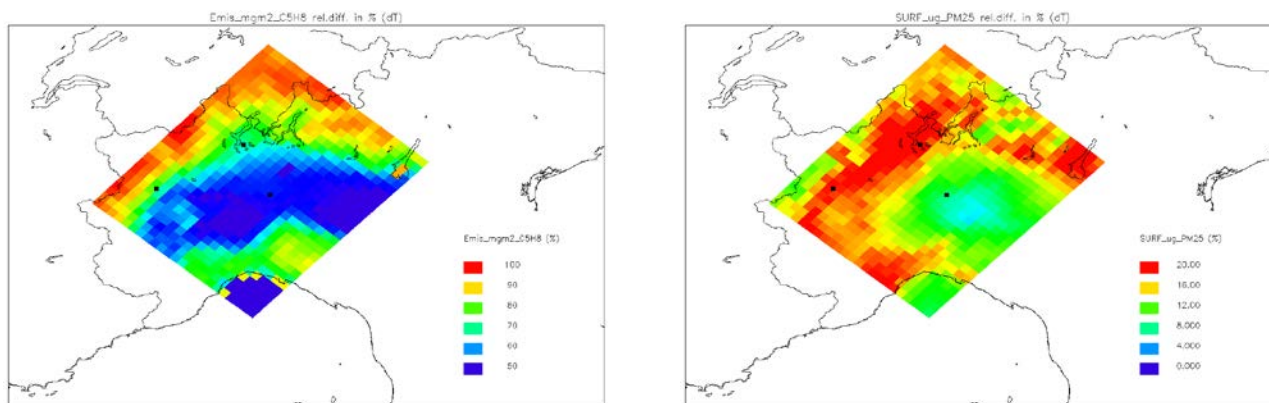


Figure 14. Modeled change in the mean concentrations for July 2006 for isoprene (left) and  $PM_{2.5}$  (right) due to a temperature increase of 5 °C. The nest with 10 km resolution is shown. Note that the color scales differ.

The results presented above indicate small differences in the modeled concentrations of ozone and aerosols for different spatial resolutions and model nests. This should not, however, be seen as an indication that the modeled SOA and ozone are very robust and independent on meteorological drivers. Figure 15 shows the modeled BSOA for two types of meteorological models (HIRLAM and WRF) and two types of land use (EMEP and Modis) for the point in the Torino area. Substantial differences in the BSOA concentrations are found, indicating a large degree of uncertainty for this compound. The main reason for the large differences in BSOA seen in Figure 15 is due to differences in precipitation. In general, the EMEP meteorology (HIRLAM) produces much more precipitation than some of the WRF schemes, thus causing a more effective washout of the aerosols. Different types of land use had, however, fairly small effect on the modeled BSOA.

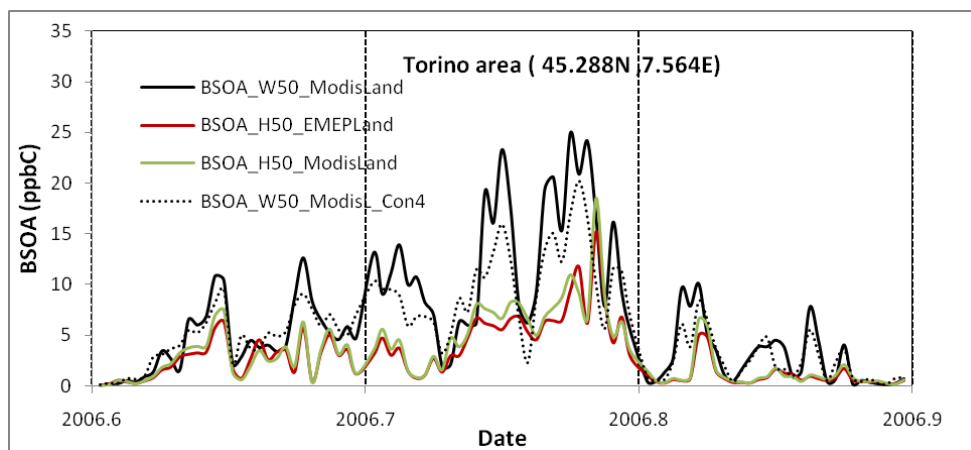


Figure 15. Hourly concentrations of BSOA for a point in the Torino area as modeled with the 10 km nest for June-August 2006. The time series show the concentrations with different types of land use data (ModisLand and EMEPLand) and meteorological data. 'W50' = WRF50 km, 'H50' = Hirlam 50 km, 'Con4' is an alternative version of WRF with more convection.

## 1.5 Summary

Model calculations for the heat waves in the East Mediterranean megacity hot spot area in summer 2007 are presented using the WRF-Chem and the EMEP Unified models. Whereas there is a lack of relevant surface monitoring sites in this area, satellite data for the tropospheric columns of  $NO_2$

agrees fairly well the model calculations. The heat waves lead to numerous wild fires in the region. The fire plumes were seen by satellite instruments and are also reflected fairly well in the models.

Emissions of biogenic VOCs (isoprene and terpenes) reacting with the megacity anthropogenic  $\text{NO}_x$  emissions are calculated to contribute significantly to the levels of ozone and secondary organic aerosols in the region. Furthermore, the WRF-Chem/MEGAN model gives considerably higher emissions of biogenic isoprene than the EMEP Unified model. High temperatures were seen to influence ozone through the emissions of biogenic isoprene.

Model studies for the Po Valley hot spot using a nested EMEP/WRF model system are also presented. A modeling system nesting down from the standard 50 km to 2.5 km, including state-of-the-art modules for BVOC emissions and secondary organic aerosol (SOA) formation is used for the first time as part of CityZen. With the meteorological and land use data applied here we found certain differences when zooming down from 50 km to 10 km, whereas there were less differences between the 10 km and 2.5 km results for BSOA.

Temperature showed to have a significant effect on the formation of  $\text{O}_3$ , PM and SOA in the Po Valley area as calculated with the nested EMEP/WRF system. An increase of  $5^\circ\text{C}$  lead to an overall increase of 40 % BSOA in the whole area, and an increase of around 20 % in the  $\text{PM}_{2.5}$  concentration north of the Po Valley. For  $\text{PM}_{2.5}$  smaller effects were seen inside the Po Valley basin itself, presumably reflecting the smaller biogenic emissions given by the EMEP Unified model there.

The type of models and meteorological data applied is shown to have a decisive influence on the modelled SOA. Sensitivity runs with different meteorological processes in the WRF model gave substantial differences in the results. Thus, the influence of the mixing of biogenic VOCs with anthropogenic  $\text{NO}_x$  from the megacities for the ozone and aerosols formed is subject to very large uncertainties. This is partly explained by uncertainties in condensation, precipitation and washout and partly due to uncertain biogenic emissions.

## 1.6 Acknowledgements

The authors would like to acknowledge Hugo A. C. Denier van der Gon at TNO Built Environment and Geosciences for access to the TNO/EMEP anthropogenic emission data set. We are also thankful to Solene Turquety at Laboratoire de Météorologie Dynamique for providing IASI satellite observations. David Simpson and Peter Wind at the Norwegian Meteorological Institute (met.no) are acknowledged for their invaluable help and assistance with the EMEP Unified model. Philippe Thunis at JRC/Ispra is acknowledged for giving us access to the POMI emission data.

## 1.7 Technical Appendix: Biogenic emissions and routines for secondary organic aerosols (SOA) in the EMEP model

In parallel with CityZen a development of routines for biogenic emissions and formation of secondary organic aerosols (SOA) were carried out as part of the EMEP model development. This was closely connected with WP2.2 in CityZen and an overview of the theory and work is given below.

### 1. Foliar BVOC emissions

In the EMEP model biogenic emissions of isoprene and monoterpenes are calculated for every grid-cell, and at every model timestep, using near-surface air temperature ( $T_2$ ) and photosynthetically active radiation (PAR), the latter being calculated from the model's solar radiation, modified by the total cloud fraction (CL). Following the ideas proposed in e.g. Guenther et al. (1993, 1995), the first step in the emission processing is to define 'standard' emission factors  $E_{\lambda_c,i}^*$ , which give the emissions of particular land-covers at standard environmental conditions (30°C and photosynthetically active radiation of 1000  $\mu\text{mole m}^{-2}\text{s}^{-1}$ ).

Emission factors for forests have been created from the map of forest species generated by Köble and Seufert (2001). This work provided maps for 115 tree species in 30 European countries, based upon a compilation of data from the ICP-forest network UNECE (1998). The EMEP model cannot deal with all these different forest species, but rather has maps of aggregated landcover types, such as temperate/boreal coniferous forest (CF). Emission rates for the EMEP aggregated land-cover classes ( $\Lambda_c$ ) are developed from maps of the real landcover types ( $\lambda_c$ ) with:

$$E_{\Lambda_c,i}^* = \frac{\sum_{\lambda_c} \varepsilon_{\lambda_c,i} A_{\lambda_c} D_{\lambda_c} \delta(\lambda_c \in \Lambda_c)}{\sum_{\lambda_c} A_{\lambda_c}}$$

where  $E_{\Lambda_c,i}^*$  is the area-specific reference emission rate ( $\mu\text{g/m}^2/\text{h}$ ) for an EMEP landcover class ( $\Lambda_c$ ), at standard environmental conditions,  $\varepsilon_{\lambda_c,i}$  is the mass-specific emission rate ( $\mu\text{g/g}(\text{dry-weight})/\text{h}$ ) for BVOC compound  $i$  and a particular real landcover class ( $\lambda_c$ ) at these standard conditions,  $A_{\lambda_c}$  is the area, and  $D_{\lambda_c}$  is the foliar biomass density of that species. The  $\delta$  function is used to include only those species ( $\lambda_c$ ) belonging to the EMEP landcover group ( $\Lambda_c$ ). Emission potentials are then recalculated to instantaneous emissions every time-step in the model, using the grid-cell relevant temperature and radiation conditions:

$$E_{\Lambda_c,i} = E_{\Lambda_c,i}^* \times A_{\Lambda_c} \times \gamma_{\Lambda_c,i}$$

Where now  $E_{\Lambda_c,i}$  is the temperature and (where appropriate) light corrected emission per square meter of EMEP landcover  $\Lambda_c$ . The environmental correction factor  $\gamma_{\Lambda_c,i}$  consists of corrections for the canopy foliar mass, temperature and light:

$$\gamma_{\Lambda_c,i} = \gamma_{LAI} \times \gamma_L \times \gamma_{T,i}$$

The EMEP model deals with three emission categories ( $i$ ):

- iso: Isoprene,  $\gamma_L$  and  $\gamma_{T,iso}$  as in Guenther et al. (1993)
- mtp: Pool-dependent monoterpene emissions, use simple exponential  $\gamma_{T,mtp}$  from Guenther et al. (1993).
- mtl: Light-dependent monoterpene emissions, use simple exponential  $\gamma_{T,mtl}$  from Guenther et al. (1993).

The LAI factor,  $\gamma_{LAI}$  is simply defined as  $LAI/LAI_{max}$  for each land-cover  $\Lambda_c$ . The light correction factor  $\gamma_L$  and temperature correction factor  $\gamma_T$  are as given in Guenther et al. (1993) and Simpson et al. (1995). Isoprene is always light and temperature controlled. A fraction of monoterpenes (denoted MTP) are derived entirely from pool-emissions, and so have  $\gamma_L = 1$  always. These MTP emissions use the simple exponential form. Some monoterpene emissions (MTL) are synthesised, and are both light and temperate controlled.

## 2. EMEP VBS/SOA module

The EMEP MSC-W chemical transport model (Simpson et al., 2007) has been extended with a new organic aerosol (OA) scheme based on the Volatility Basis Set (VBS) approach (Donahue et al., 2006). The VBS framework describes OA by separating low volatility organics into decadal spaced bins of saturation concentration ( $C_i^*$ ) between 0.01 and  $10^6 \mu\text{g m}^{-3}$ .  $C_i^*$  is proportional to the vapor pressure and is a semi-empirical property that describes the gas-particle partitioning of an organic mixture (Pankow, 1994). Each  $C_i^*$  bin contains species that span a range of volatilities, i.e. the  $1 \mu\text{g m}^{-3}$  bin contains species with  $C_i^*$  between  $0.3 \mu\text{g m}^{-3}$  and  $3 \mu\text{g m}^{-3}$ . The lowest volatility bin,  $0.01 \mu\text{g m}^{-3}$ , contains all species lower in volatility than  $0.03 \mu\text{g m}^{-3}$ . The  $C_i^*$  spectrum is conventionally divided into semi-volatile (SVOC,  $0.01 - 10^3 \mu\text{g m}^{-3}$ ) and intermediate volatility (IVOC,  $10^4 - 10^6 \mu\text{g m}^{-3}$ ) organic compounds.

The EMEP model includes the following basis set (bins) for primary organic aerosols (POA):

$$\{C_i^*\} = \{0.01, 0.1, 1, 10, 100, 1000, 10\,000, 100\,000, 1000\,000\} \mu\text{g m}^{-3}$$

and four groups for secondary organic aerosols (SOA):

$$\{C_i^*\} = \{1, 10, 100, 1000\} \mu\text{g m}^{-3}$$

It is assumed that ambient OA exists in equilibrium between the gas and particle phases as dictated by Raoult's law and that the organics in the particle phase form a pseudo-ideal solution (Pankow, 1994). The gas-aerosol partitioning equation can be described as (Donahue et al., 2006):

$$\xi_i = \left(1 + \frac{C_i^*}{C_{OA}}\right)^{-1}; C_{OA} = \sum_i C_i \xi_i$$

where  $\xi_i$  is the fraction of organic mass in volatility bin  $i$  that exists in particulate phase,  $C_i^*$  is the effective saturation concentration of bin  $i$ ,  $C_{OA}$  is the total particulate OA (POA + SOA) concentration, and  $C_i$  is the total organic concentration (gas + particle) in bin  $i$  ( $\mu\text{g m}^{-3}$ ). If  $C_{OA}$  is  $1.0 \mu\text{g m}^{-3}$  and a given compound has  $C_i^* = 1 \mu\text{g m}^{-3}$  we would expect 50% of the mass of that compound to be found in the condensed phase and 50% in the gas/vapor phase. Shifts in gas-particle partitioning due to changes in temperature are represented using the Clausius-Clapeyron equation (Donahue et al., 2006)

$$C_i^*(T) = C_i^*(T_{ref}) \exp \left[ \frac{\Delta H_v}{R} \left( \frac{1}{T_{ref}} - \frac{1}{T} \right) \right] \frac{T_{ref}}{T}$$

where  $T_{ref}$  is the reference temperature (298 K),  $\Delta H_v$  is the heat of vaporization and  $R$  is the universal gas constant.

The current version of the EMEP model also includes aging of Primary Organic Aerosol (POA) emissions, described by Shrivastava et al. (2008). Aging proceeds by a first-order reaction of VBS vapors with OH radicals producing a product that has a  $C_i^*$  one order of magnitude lower than its precursor. We assume that the oxidation products in the vapor phase continue to age and form even lower volatility products. Primary organic compounds are assumed to age with a reaction rate of

$4 \times 10^{-11} \text{ cm}^3 \text{ molecule}^{-1} \text{ s}^{-1}$  whereas secondary organic compounds have a reaction rate of  $k = 4 \times 10^{-12} \text{ cm}^3 \text{ molecule}^{-1} \text{ s}^{-1}$ .

It should be mentioned that total POA/IVOC emissions are assumed to be 2.5 times larger than the “traditional” estimates using inert POA, but most of the direct emissions are in the gaseous phase.

## 1.8 References

Colette, A., Granier, C., Hodnebrog, Ø., Jakobs, H., Maurizi, A., Nyiri, A., Bessagnet, B., D'Angiola, A., D'Isidoro, M., Gauss, M., Meleux, F., Memmesheimer, M., Mieville, A., Rouil, L., Russo, F., Solberg, S., Stordal, F., and Tampieri, F.: Air quality trends in Europe over the past decade: a first multi-model assessment, *Atmos. Chem. Phys. Discuss.*, 11 (7), 19029-19087, 10.5194/acpd-11-19029-2011, 2011.

Curci G., Beekmann M., Vautard R. et al.: Modelling study of the impact of isoprene and terpene biogenic emissions on European ozone levels, *Atmos. Environ.* 43 (7), 1444-1455, doi: 10.1016/j.atmosenv.2008.02.070, 2009.

Donahue, N. M., et al., The coupled partitioning, dilution and chemical aging of semivolatile organics. *Environmental Science & Technology* 40(8), 2635-2643, 2006.

Dore, C. J., Watterson, J. D., Murrells, T. P., Passant, N. R., Hobson, M. M., Choudrie, S. L., Thistlethwaite, G., Wagner, A., Jackson, J., Li, Y., Bush, T., King, K. R., Norris, J., Coleman, P. J., Walker, C., Stewart, R. A., Goodwin, J. W. L., Tsagatakis, I., Conolly, C., Downes, M. K., Brophy, N., and Hann, M. R.: UK Emissions of Air Pollutants 1970 to 2005, Technical Report, 2007.

Emmerson, K. M., Carslaw, N., Carslaw, D. C., Lee, J. D., McFiggans, G., Bloss, W. J., Gravestock, T., Heard, D. E., Hopkins, J., Ingham, T., Pilling, M. J., Smith, S. C., Jacob, M., and Monks, P. S.: Free radical modelling studies during the UK TORCH Campaign in Summer 2003, *Atmos. Chem. Phys.*, 7, 167-181, doi:10.5194/acp-7-167-2007, 2007.

Eremenko, M., Dufour, G., Foret, G., Keim, C., Orphal, J., Beekmann, M., Bergametti, G., and Flaud, J. M.: Tropospheric ozone distributions over Europe during the heat wave in July 2007 observed from infrared nadir spectra recorded by IASI, *Geophys. Res. Lett.*, 35 (18), 10.1029/2008gl034803, 2008.

Founda, D., and Giannakopoulos, C.: The exceptionally hot summer of 2007 in Athens, Greece - A typical summer in the future climate?, *Glob. Planet. Change*, 67 (3-4), 227-236, 10.1016/j.gloplacha.2009.03.013, 2009.

Gerasopoulos, E., Kouvarakis, G., Vrekoussis, M., Kanakidou, M., and Mihalopoulos, N.: Ozone variability in the marine boundary layer of the eastern Mediterranean based on 7-year observations, *J. Geophys. Res.-Atmos.*, 110 (D15), D15309, doi: 10.1029/2005jd005991, 2005.

Grell, G. A., et al., Fully coupled "online" chemistry within the WRF model, *Atmospheric Environment*, 39 (37), 6957-6975, 2005.

Guenther, A., et al., Isoprene and monoterpene rate variability: Model evaluations and sensitivity analysis, *J. Geophys. Res.*, Vol. 98, No.10, page 12609-12617, 1993.

Guenther, A., et al., A global model of natural volatile organic compound emissions, *J. Geophys. Res.*, 100, 8873-8892, 1995.

Guenther, A., Karl, T., Harley, P., Wiedinmyer, C., Palmer, P. I., and Geron, C.: Estimates of global terrestrial isoprene emissions using MEGAN (Model of Emissions of Gases and Aerosols from Nature), *Atmospheric Chemistry and Physics*, 6, 3181-3210, 2006.

- Hodnebrog, Ø., Stordal, F., and Berntsen, T. K.: Does the resolution of megacity emissions impact large scale ozone?, *Atmospheric Environment*, In Press, Corrected Proof, 10.1016/j.atmosenv.2011.01.012, 2011a.
- Hodnebrog, Ø., Solberg, S., Stordal F., Svendby, T., et al.: A model study of the Eastern Mediterranean ozone levels during the summer of 2007, *Atmospheric Chemistry and Physics*, to be submitted, 2011b.
- Kanakidou, M., Mihalopoulos, N., Kindap, T., Im, U., Vrekoussis, M., Gerasopoulos, E., Dermizaki, E., Unal, A., Koçak, M., Markakis, K., Melas, D., Kouvarakis, G., Youssef, A. F., Richter, A., Hatzianastassiou, N., Hilboll, A., Ebojie, F., Wittrock, F., von Savigny, C., Burrows, J. P., Ladstaetter-Weissenmayer, A., and Moubasher, H.: Megacities as hot spots of air pollution in the East Mediterranean, *Atmospheric Environment*, 45 (6), 1223-1235, 10.1016/j.atmosenv.2010.11.048, 2011.
- Kaskaoutis, D. G., Kharol, S. K., Sifakis, N., Nastos, P. T., Sharma, A. R., Badarinath, K. V. S., and Kambezidis, H. D.: Satellite monitoring of the biomass-burning aerosols during the wildfires of August 2007 in Greece: Climate implications, *Atmospheric Environment*, 45 (3), 716-726, 10.1016/j.atmosenv.2010.09.043, 2011.
- Kuenen J., H. Denier van der Gon, A. Visschedijk, H. van der Brugh, S. Finardi, P. Radice, A. d'Allura, S. Beevers, J. Theloke, M. Uzbasich, C. Honoré, O. Perrussel (2010): A Base Year (2005) MEGAPOLI European Gridded Emission Inventory (Final Version). Deliverable D1.6, MEGAPOLI Scientific Report 10-17, MEGAPOLI-20-REP-2010-10, 39p, 2010.
- Köble, R. and Seufert, G.: Novel maps for forest tree species in Europe, in: A changing atmosphere: 8th European symposium on the physico-chemical behaviour of atmospheric pollutants, Torino, 2001.
- Liu, Y., Kahn, R. A., Chaloulakou, A., and Koutrakis, P.: Analysis of the impact of the forest fires in August 2007 on air quality of Athens using multi-sensor aerosol remote sensing data, meteorology and surface observations, *Atmospheric Environment*, 43 (21), 3310-3318, 10.1016/j.atmosenv.2009.04.010, 2009.
- Madronich, S.: Photodissociation in the atmosphere .1. Actinic flux and the effects of ground reflections and clouds, *J. Geophys. Res.-Atmos.*, 92 (D8), 9740-9752, 1987.
- Pankow, J. F., An Absorption-Model of Gas-Particle Partitioning of Organic-Compounds in the Atmosphere, *Atmospheric Environment* 28(2), 185-188, 1994.
- Poupkou, A., Symeonidis, P., Lisaridis, I., Melas, D., Ziomas, I., Yay, O. D., and Balis, D.: Effects of anthropogenic emission sources on maximum ozone concentrations over Greece, *Atmospheric Research*, 89 (4), 374-381, 10.1016/j.atmosres.2008.03.009, 2008.
- Poupkou, A., Melas, D., Ziomas, I., Symeonidis, P., Lisaridis, I., Gerasopoulos, E., and Zerefos, C.: Simulated Summertime Regional Ground-Level Ozone Concentrations over Greece, *Water Air Soil Pollut.*, 196 (1-4), 169-181, 10.1007/s11270-008-9766-0, 2009.
- Shrivastava, M.K, et al., Effects of Gas-Particle Partitioning and Aging of Primary Emissions on Urban and Regional Organic Aerosol Concentrations, *Journal of Geophysical Research* 113, D18301, DOI:10.1029/2007JD009735, 2008.
- Simpson D., et al., Biogenic emissions in Europe. *J. Geophys. Res.*, 100, 22 875 - 22 890, 1995.
- Simpson, D., Winiwarter, W., Borjesson, G., Cinderby, S., Ferreiro, A., Guenther, A., Hewitt, C. N., Janson, R., Khalil, M. A. K., Owen, S., Pierce, T. E., Puxbaum, H., Shearer, M., Skiba, U., Steinbrecher, R., Tarrason, L., and Oquist, M. G.: Inventorying emissions from nature in Europe, *J. Geophys. Res.-Atmos.*, 104 (D7), 8113-8152, 1999.

- Simpson, D., et al., The EMEP Unified Eulerian Model. Model Description. EMEP MSC-W Report 1/2003, The Norwegian Meteorological Institute, Oslo, Norway, 2003.
- Simpson, D., Ashmore, M. R., Emberson, L., and Tuovinen, J. P.: A comparison of two different approaches for mapping potential ozone damage to vegetation. A model study, *Environ. Pollut.*, 146 (3), 715-725, 10.1016/j.envpol.2006.04.013, 2007.
- Skamarock, W. C., and Klemp, J. B., A time-split nonhydrostatic atmospheric model for weather research and forecasting applications, *J. Comput. Phys.*, 227 (7), 3465-3485, 10.1016/j.jcp.2007.01.037, 2008.
- Solberg, S., Ø. Hov, A. Søvde, I. S. A. Isaksen, P. Coddeville, H. De Backer, C. Forster, Y. Orsolini, and K. Uhse (2008), European surface ozone in the extreme summer 2003, *J. Geophys. Res.*, 113, D07307, doi:10.1029/2007JD009098.
- Stockwell, W. R., et al., The 2nd generation regional acid deposition model chemical mechanism for regional air-quality modeling, *J. Geophys. Res.-Atmos.*, 95 (D10), 16343-16367, 1990.
- Symeonidis, P., Poupkou, A., Gkantou, A., Melas, D., Yay, O. D., Pouspourika, E., and Balis, D.: Development of a computational system for estimating biogenic NMVOCs emissions based on GIS technology, *Atmospheric Environment*, 42 (8), 1777-1789, 10.1016/j.atmosenv.2007.11.019, 2008.
- Søvde, O. A., Gauss, M., Smyshlyaev, S. P., and Isaksen, I. S. A.: Evaluation of the chemical transport model Oslo CTM2 with focus on arctic winter ozone depletion, *J. Geophys. Res.-Atmos.*, 113 (D9), 10.1029/2007jd009240, 2008.
- Thunis, P., et al, Air pollution and emission reductions over the Po-valley: Air quality modelling and integrated assessment, 18th world IMACS congress and MODSIM09 international congress on modeling and simulation: Interfacing modeling and simulation with mathematical and computational sciences, pp. 2335-2341, 2009.
- Tressol, M., Ordonez, C., Zbinden, R., Brioude, J., Thouret, V., Mari, C., Nedelec, P., Cammas, J.-P., Smit, H., Patz, H.-W., and Volz-Thomas, A.: Air pollution during the 2003 European heat wave as seen by MOZAIC airliners, *Atmos. Chem. Phys.*, 8, 2133-2150, doi:10.5194/acp-8-2133-2008, 2008.
- Turquety, S., Hurtmans, D., Hadji-Lazaro, J., Coheur, P. F., Clerbaux, C., Josset, D., and Tsamalis, C.: Tracking the emission and transport of pollution from wildfires using the IASI CO retrievals: analysis of the summer 2007 Greek fires, *Atmos. Chem. Phys.*, 9 (14), 4897-4913, 2009.
- UNECE: International Co-operative Programme an Assessments and Monitoring of Air Pollution Effects on Forests. Manual on methods and criteria for harmonized sampling, assessment, monitoring and analysis of the effects of air pollution on forest, 1998.
- van der Werf, G. R., Randerson, J. T., Giglio, L., Collatz, G. J., Kasibhatla, P. S., and Arellano, A. F.: Interannual variability in global biomass burning emissions from 1997 to 2004, *Atmospheric Chemistry and Physics*, 6, 3423-3441, 2006.
- Vieno, M., Dore, A. J., Stevenson, D. S., Doherty, R., Heal, M. R., Reis, S., Hallsworth, S., Tarrason, L., Wind, P., Fowler, D., Simpson, D., and Sutton, M. A.: Modelling surface ozone during the 2003 heat-wave in the uk, *Atmos. Chem. Phys.*, 10, 7963-7978, 10.5194/acp-10-7963-2010.
- Wiedinmyer, C., Akagi, S. K., Yokelson, R. J., Emmons, L. K., Al-Saadi, J. A., Orlando, J. J., and Soja, A. J.: The Fire INventory from NCAR (FINN): a high resolution global model to estimate the emissions from open burning, *Geosci. Model Dev.*, 4 (3), 625-641, 10.5194/gmd-4-625-2011, 2011.
- Ziemke, J. R., Chandra, S., Duncan, B. N., Froidevaux, L., Bhartia, P. K., Levelt, P. F., and Waters, J. W.: Tropospheric ozone determined from aura OMI and MLS: Evaluation of measurements and comparison with the Global Modeling Initiative's Chemical Transport Model, *J. Geophys. Res.-Atmos.*, 111 (D19), D19303, doi: 10.1029/2006jd007089, 2006.